ACSNANO
www.acsnano.org
ARTICLE

Single-Molecule DNA Methylation Quantification Using Electro-optical Sensing in Solid-State Nanopores

Tal Gilboa,[†,#] Chen Torfstein,[†,#] Matyas Juhasz,[‡] Assaf Grunwald,[§] Yuval Ebenstein,[*,§] Elmar Weinhold,[‡] and Amit Meller[*,†,∥]

[†]Department of Biomedical Engineering, The Technion−Israel Institute of Technology, Haifa, 32000 Israel
[‡]Institute of Organic Chemistry, RWTH Aachen University, Landoltweg 1, D-52056 Aachen, Germany
[§]Raymond and Beverly Sackler Faculty of Exact Sciences, School of Chemistry, Tel Aviv University, Tel Aviv, 6997801 Israel
[∥]Department of Biomedical Engineering, Boston University, Boston, Massachusetts 02215, United States

Supporting Information

ABSTRACT: **Detection of epigenetic markers, including 5-methylcytosine, is crucial due to their role in gene expression regulation and due to the mounting evidence of aberrant DNA methylation patterns in cancer biogenesis. Single-molecule methods to date have primarily been focused on hypermethylation detection; however, many oncogenes are hypomethylated during cancer development, presenting an important unmet biosensing challenge. To this end, we have developed a labeling and single-molecule quantification method for multiple unmethylated cytosine−guanine dinucleotides (CpGs). Our method involves a single-step covalent coupling of DNA with synthetic cofactor analogues using DNA methyltransferases (MTases) followed by molecule-by-molecule electro-optical nanopore detection and quantification with single or multiple colors. This sensing method yields a calibrated scale to directly quantify the number of unmethylated CpGs in the target sequences of each DNA molecule. Importantly, our method can be used to analyze ∼10 kbp long double-stranded DNA while circumventing PCR amplification or bisulfite conversion. Expanding this technique to use two colors, as demonstrated here, would enable sensing of multiple DNA MTases through orthogonal labeling/sensing of unmethylated CpGs (or other epigenetic modifications) associated with specific recognition sites. Our proof-of-principle study may permit sequence-specific, direct targeting of clinically relevant hypomethylated sites in the genome.**

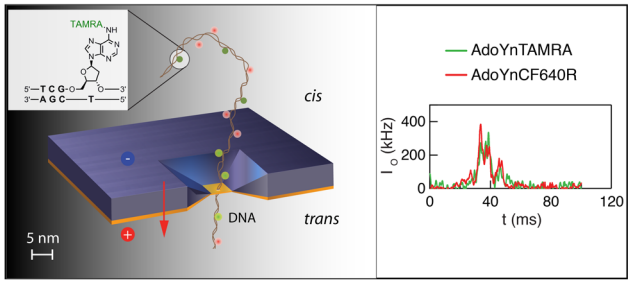

KEYWORDS: *5-methylcytosine, epigenetic modifications, solid-state nanopores, metyltransferase, single-molecule, electro-optical sensing*

In the human genome about 60−80% of all cytosine−guanine dinucleotides (CpGs) are methylated. Methylation state plays extremely important roles in regulation of gene expression.[1,2] Specifically, aberrant DNA methylation levels have been associated with various types of cancers, where tumor suppressor genes, such as p53, are hypermethylated, leading to gene silencing, while many oncogenes are hypomethylated to promote their overexpression. Moreover, large cell-to-cell variations in methylation patterns indicate that intratumoral heterogeneity plays a critical role in tumor progression, while highly complicating bulk analysis of methylation patterns.[3,4] Despite the growing evidence supporting the need for quantification of DNA methylation patterns, the availability of quantitative methods for sensing these genomic modifications, particularly at the single-molecule level, has remained to date limited.[5] Unlike the DNA primary sequence, chemical DNA modifications are not preserved in DNA amplification, complicating sensing of epigenetic markers. Furthermore, bulk sensing methods often require averaging across thousands of DNA fragments, a process that limits the ability to detect heterogeneity within tumors. To overcome these limitations and enable simple and efficient single-cell epigenetic profiling, single-molecule sensing technologies have been recently developed, such as SMRT sequencing, although this method involves large and expensive instrumentation.[6,7]

Nanopores (NPs) represent an emerging single-molecule analysis technique capable of probing the structure of complex biological molecules and their interactions with other biomolecules.[8−10] In the nanopore system an electrical field is

Received: July 16, 2016
Accepted: August 31, 2016
Published: August 31, 2016

DOI: 10.1021/acsnano.6b04748
ACS Nano 2016, 10, 8861−8870

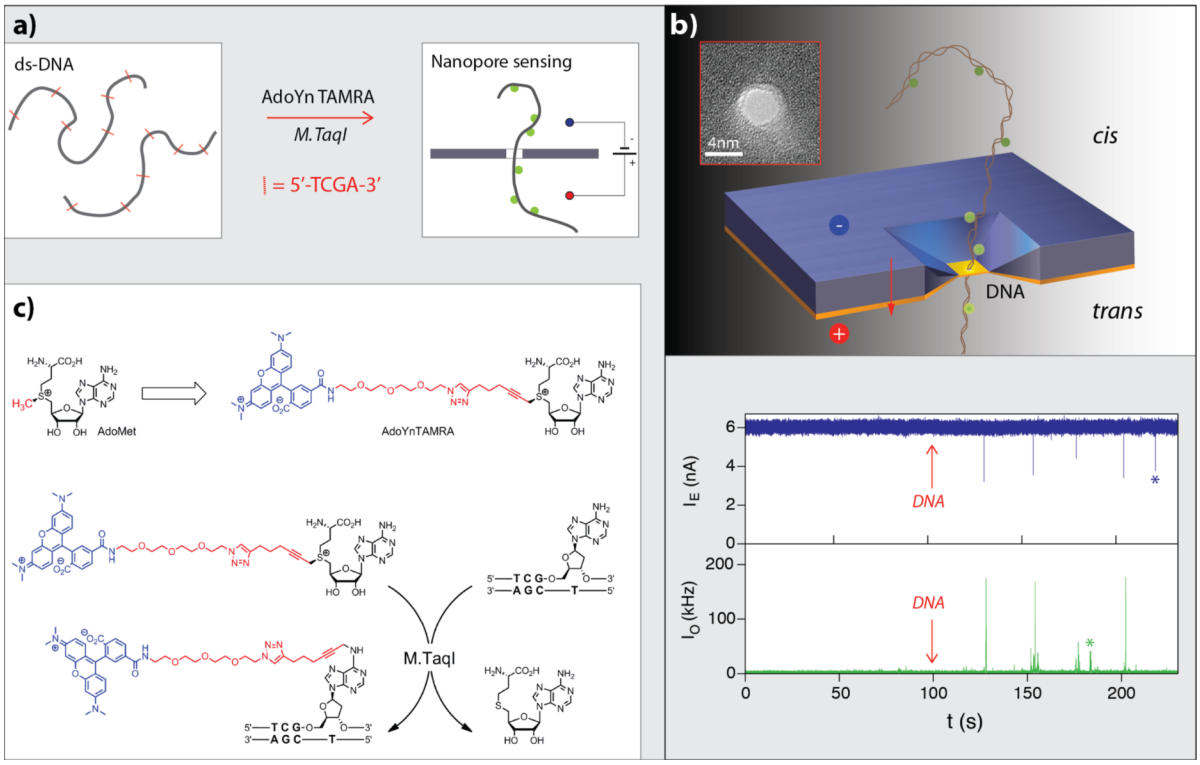

Figure 1. One-step enzymatic method coupled to electro-optical nanopore sensing for quantification of DNA methylation at the single-molecule level. (a) Schematic illustration of our method. Double-stranded DNA is reacted with DNA MTase and custom-made AdoMet analogues equipped with a fluorescent moiety. The labeled DNA molecules are then analyzed one by one using a nanopore device. (b) The DNA readout process involves threading of the linearized DNA through a solid-state nanopore roughly 4 nm in diameter, as shown in the TEM micrograph (inset). The nanopore ion current and the fluorescence emissions are interrogated simultaneously. Entries of labeled 10 kbp DNA molecules are recorded as a simultaneous downward spike in the ion current and upward photon bursts, as shown in the lower panel. Photon spikes not associated with DNA translocations are readily observed and rejected (marked with a green asterisk). (c) M.*Taq*I catalyzes the transfer of the extended side chain from the synthetic cofactor analogue AdoYnTAMRA to the amino group of adenine with the double-stranded 5′-TCGA-3′ DNA sequence, leading to fluorescently labeled DNA and the cofactor product *S*-adenosyl-L-homocystein.

used to mobilize an electrically charged biopolymer toward and through a nanoscale aperture. When the biopolymer is threaded through the pore, it blocks a fraction of the ionic current that flows through it, resulting in an ion current blockade event. Since the molecules are threaded in a single-file manner, this method enables direct scanning of useful molecular features along long biopolymers. For example, engineered protein nanopores, such as the MspA channel, have been developed for direct DNA sequencing of long DNA strands.[11−13] Furthermore, solid-state NP (ssNPs) have been fabricated with subnanometer precision to match the size (the cross-section) of many target analytes,[14,15] enabling additional biosensing applications such as DNA barcoding of pathogens,[16] mapping binding of transcription factors to their DNA targets,[17] and label-free identification of single nucleotides,[18] to name a few. To detect epigenetic biomarkers including 5-methylcytosine (5 mC) or 5-hydroxymethylcytosine (5 hmC), bulky groups, such as methyl-CpG-binding domain (MBD) proteins or streptavidin, were conjugated to the DNA in order to produce an observable ion current blockade on top of the blockade level of the bare DNA.[19,20] This method is appealing in its simplicity, but may not be used to probe densely methylated regions in the genome, due to the bulkiness of the conjugated proteins. Furthermore, to date, direct NP quantification of unmethylated 5-methylcytosine sites has not been reported.

To enable hypomethylation quantification, we have developed an electro-optical ssNP sensing method to probe unmethylated CpG sites in kbp long double-stranded DNA (dsDNA) molecules. Single-molecule fluorescence sensing can substantially expand the range of NP sensing applications while offering a highly parallel platform with broad signal bandwidth.[21−26] Recently, single-molecule fluorescence sensing has been employed for the detection of short, self-quenched molecular beacons threaded through a ssNP.[27] In the current study, we have employed electro-optical sensing in ssNPs to directly detect sequence-specific methylation in long DNA molecules. Moreover, we show that the emitted photons' intensity just before and after the passage of each DNA molecule through the ssNP quantitatively correlates with the number of unmethylated CpGs in the DNA target, regardless of the NP size or the actual dwell time of each molecule in the NP device.

Our method involves a one-step enzymatic reaction, using DNA methyltransferases (MTases) with small molecular weight synthetic cofactors to directly conjugate fluorescent probes to unmethylated CpG sites. An ultrasensitive electro-optical nanopore sensing tool, which permits single-fluorophore, multicolor quantification, is then applied to produce highly quantitative single-molecule fluorescence measurements. In our system two independent, time-resolved measurements take place simultaneously during the threading and passage of each DNA molecule through a ssNP: (i) an electrical ion current measurement, acting as a gate signal that reports the dwell time of each DNA molecule in the pore, regardless of whether it is

DOI: 10.1021/acsnano.6b04748
ACS Nano 2016, 10, 8861−8870

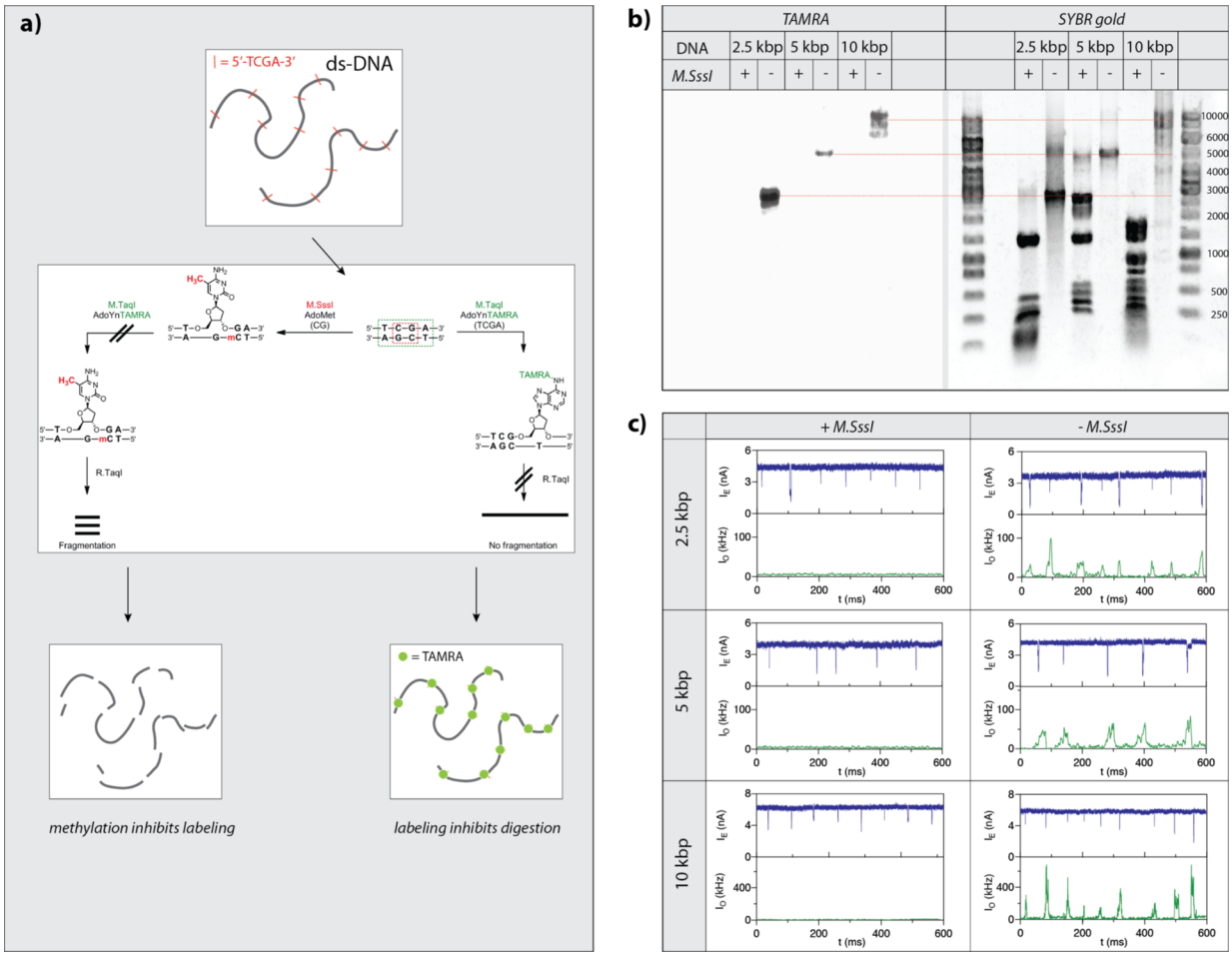

Figure 2. Bulk and single-molecule validation of M.*Taq*I labeling using custom AdoYnTAMRA. (a) Schematic representation of the biochemical assay: DNA samples containing known numbers of M.*Taq*I recognition sites (5′-TCGA-3′) are split into two: one-half (left branch) is treated with M.SssI DNA MTase in the presence of native AdoMet, and the second half (right branch) is kept in its original unmethylated state. After purification of the methylated sample, both samples are then incubated with M.*Taq*I and AdoYnTAMRA under equal conditions. The DNA samples are then challenged with the REase R.*Taq*I, which cleaves unmethylated and CpG-methylated 5′-TCGA-3′ sequences but leaves A-modified 5′-TCGA-3′ sequences intact. (b) Analysis of 2.5, 5, and 10 kbp DNA, either pretreated with M.SssI/AdoMet or not prior to the incubation with M.*Taq*I/AdoYnTAMRA, by R.*Taq*I. Syber Gold staining of the DNA (right panel) shows that only the CpG-methylated fragments were digested. TAMRA excitation (left panel) shows single bands for the unmethylated −M.SssI samples. Together these gels validate the activity of the M.*Taq*I/AdoYnTAMRA as expected. (c) Representative electro-optical traces of the six DNA samples as in panel b. Optical signals are observed only for the unmethylated −M.SssI samples.

labeled or not, and (ii) a high-sensitivity single-molecule fluorescence readout for single or multiple colors, which is used to quantify the unmethylated CpG sites in specific DNA recognition sequences. Notably, our method is generalizable to many DNA MTases targeting multiple specific sequences, each coupled to its own color-encoded probe.

RESULTS AND DISCUSSION

Electro-optical Sensing of Methyltransferase-Coupled Fluorophores. DNA MTases catalyze the transfer of the activated methyl group from the natural cofactor *S*-adenosyl-L-methionine (AdoMet) to the C5 or N4 position of cytosine or the N6 position of adenine, within specific double-stranded DNA sequences ranging from two to eight base pairs.[28] The catalytic repertoire of DNA MTases has been extended with synthetic AdoMet analogues used for functionalization and labeling of DNA.[29] Here, we synthesized and used double-activated AdoMet analogues, which contain extended unsaturated side chains instead of a methyl group at the sulfonium center. The extended side chain, which replaces the methyl group in AdoMet, reduces the reaction rate of the transfer by the MTase due to unfavorable steric effects within the transition state. In order to accelerate the reaction rate, a triple bond was placed within the transferred chain, next to the reactive carbon, which led to stabilization of the transition state and hence to a faster reaction rate.[29−31] The extended side chains in the AdoMet analogues were equipped with either the orange fluorophore TAMRA (ex. 555 nm, em. 580 nm) or the red fluorophore CF640R (ex. 642 nm, em. 662 nm). These fluorophores were selected due to their high brightness and single-molecule compatibility. To incorporate the reporter molecules, we used the DNA MTase from *Thermus aquaticus* (M.*Taq*I), which recognizes the double-stranded DNA sequence 5′-TCGA-3′ and modifies the associated adenine residue. M.*Taq*I is CpG methylation sensitive and modifies DNA only if the CpG within the recognition site is unmethylated.[32]

Our approach is illustrated schematically in Figure 1a: DNA molecules are labeled using M.*Taq*I in the presence of the

DOI: 10.1021/acsnano.6b04748
ACS Nano 2016, 10, 8861−8870

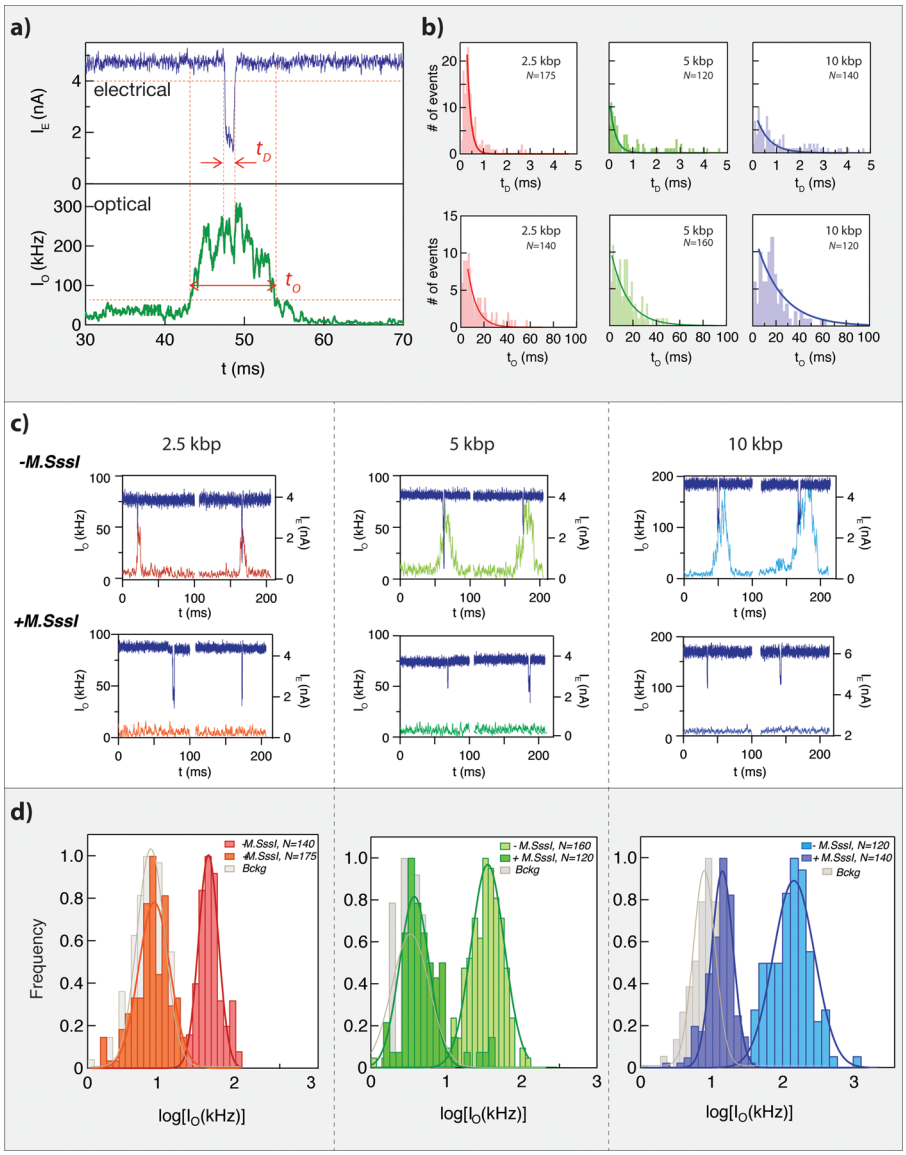

Figure 3. Detailed analysis of the electro-optical nanopore signals and DNA controls. (a) Zoom-in view of a typical DNA translocation event. The optical signals rise before the DNA enters the pore and decay after it leaves the pore. Threshold values are used to define the electrical and optical dwell times (t_D and t_O, respectively). (b) Distributions of t_D and t_O measured for the three DNA lengths. The number of events is indicated in each case. The data were approximated by exponential tail-fits to the histograms. (c) Representative electro-optical events of DNA (methylated and unmethylated) containing either 6, 7, or 21 M.*Taq*I sites (2.5, 5, and 10 kbp, respectively) as indicated either for unmethylated (−M.SssI, top) or methylated (+M.SssI, bottom). (d) Semilog histogram of the normalized photon count during the electrical dwell time for the three DNA lengths. In each case both the methylated (+M.SssI) and unmethylated (−M.SssI) samples are compared, showing at least a 5× contrast. The photon background histograms prior to DNA introduction are also shown in gray. Data are fitted by single Gaussian functions.

synthetic AdoMet analogue AdoYnTAMRA (or AdoYnCF640R).[33] After removal of residual cofactor molecules, a small DNA quantity (roughly 1 femtomole) is introduced to the *cis* chamber of our nanopore apparatus, where ion current flow and photon emission from the pore area are measured synchronously. Figure 1b depicts the nanopore sensing process (top) and shows typical time traces of electrical (blue line) and optical (green line) signals obtained using a 4 nm diameter pore before and after introducing the DNA at t = 100 s. A few seconds after the addition of the DNA, we observe discrete downward spikes (or "blockades") in the ion current (I_E), each corresponding to the translocation of an individual DNA molecule from the *cis* to *trans* chamber. The vast majority of electrical translocation events are accompanied by synchronous bursts of photons (I_O). Notably, some lower amplitude photon bursts appear even when there is no electrical blockade (an example is marked with a green asterisk). These photon bursts correspond to molecules that pass through the optical detection volume near the pore, but do not translocate through. Occasionally, we can also identify rare electrical translocation events that are not associated with photon bursts (an example is marked with a blue asterisk). These events represent either incomplete labeling by the DNA MTase or bleached fluorophores. In this study, we synchronously detect the ionic current and photon emission during DNA transport through the pore in order to circumvent inaccurate identification of DNA methylation.

DOI: 10.1021/acsnano.6b04748
ACS Nano 2016, 10, 8861−8870

Validation of the Methylation Detection Scheme. In order to validate and calibrate the DNA labeling and sensing assays, we developed a variant of the biochemical protection/restriction assay[33] for bulk and single-molecule characterizations. Our assay is depicted schematically in Figure 2a. Uniform length unmethylated DNA samples containing known numbers of M.*Taq*I recognition sites (5′-TCGA-3′) were either treated with the DNA MTase M.SssI in the presence of its native cofactor AdoMet to methylate *all* CpG dinucleotides, including those within the 5′-TCGA-3′ recognition site for M.*Taq*I (left branch), or kept in the original unmethylated state (right branch). Both samples were then incubated with M.*Taq*I and AdoYnTAMRA under identical conditions. To verify our sample preparation, we took advantage of the fact that the cognate restriction endonuclease (REase) R.*Taq*I cleaves CpG-methylated as well as unmethylated 5′-TCGA-3′ sequences, but does not restrict the DNA if the adenine within the 5′-TCGA-3′ sequences is modified. Therefore, agarose gel electrophoresis could be used to directly verify that M.*Taq*I labeled sites were not restricted by R.*Taq*I, while unlabeled samples were digested, as shown in Figure 2b.

Three different DNA molecules, roughly 2.5, 5, and 10 kbp long having 6, 7, or 21 recognition sites, respectively (Supporting Information), were chosen in order to quantify different methylation levels. Each DNA sample was treated as explained in Figure 2a and was subject to gel electrophoresis analysis. We first imaged the gel in the TAMRA channel (532 nm laser excitation and a 580 nm bandpass filter) as shown in Figure 2b, left. Then the gel was stained with SYBR Gold in order to highlight the unlabeled DNA bands (Figure 2b, right). We note that fragmentation bands appear only for the M.SssI-treated samples for all three DNA molecules, whereas the non M.SssI-treated samples remain uncut. Each of the uncut bands aligns well with a single band that appears for TAMRA emission (left panel), but the M.SssI methylated samples do not show any TAMRA labeling. These results confirm that CpG methylation blocks labeling of DNA by M.*Taq*I, providing a fluorescent reporter for the DNA methylation state. A negative control experiment showing that no labeling occurs in the absence of M.*Taq*I is presented in the Supporting Information.

Having validated the enzymatic labeling reaction with M.*Taq*I and AdoYnTAMRA, we analyzed these six DNA samples using our electro-optical nanopore device. Figure 2c shows representative electrical and optical nanopore translocation events (concatenated to preserve space) for each of the three DNA model molecules. Each DNA sample was either methylated by pretreatment with M.Sssl (left column) or left unmethylated (right column) as described above. For these experiments we used nanopores in the range of 3−5 nm diameter and laser excitation at 532 nm (120 μW). The alignment of the setup was confirmed by always starting the experiments with labeled DNA, used to fine-tune the nanopore location to yield maximal optical signals, and then washing the *cis* chamber with a clear buffer before adding the unlabeled DNAs. Our results clearly indicate that DNA methylation by M.Sssl does not affect the electrical translocation pattern (Supporting Information), but completely abolishes any photon bursts. In contrast, labeling of the native (unmethylated) DNA results in synchronized electrical blockades and photon spikes, as shown in the right column. A closer inspection of I_O for the methylated samples shows that while the optical signals are nearly flat, they are slightly above zero (average value). We attribute this small background intensity primarily to photoluminescence contribution of the thin SiN_x membrane.[27] The background emission facilitates alignment of the membrane to the confocal illumination spot, as explained in the Methods section.

The Photon Emission Rate Is Linearly Dependent on M.*Taq*I Labeling. To further quantify the electro-optical signals in our nanopore apparatus, we collected about 150 translocation events for each of the six DNA samples and performed detailed analysis of the data using a custom LabVIEW code. The ion current amplitude and the photon rate were extracted by applying two separate thresholds to the data, each one with 3 standard deviations either below the open pore current or above the optical background, respectively. These thresholds were used to automatically define the electrical dwell time of the DNA in the pore (t_D) and the optical event length (t_O) as shown in Figure 3a (see Methods and Supporting Information for further details). Since the illumination volume (defined by the confocal spot) extends beyond the nanopore membrane, we expect that always $t_O > t_D$. This expectation is borne out by our data: in Figure 3b we show the corresponding histograms of t_D (top, methylated DNA) and t_O (bottom, unmethylated DNA). Electrical event diagrams of all six samples are shown in the Supporting Information. The translocation dynamics were approximated by exponential tail-fits to the histograms, yielding the following values: 158 ± 11, 240 ± 32, and 540 ± 76 μs for the methylated 2.5, 5, and 10 kbp DNA, respectively. In contrast the total optical dwell time, which includes both the diffusion-drift time of the molecules in the vicinity of the pore and their translocation time, was more than an order of magnitude longer: 10.1 ± 1.3, 13.9 ± 1.6, and 17.4 ± 1.8 ms for the labeled 2.5, 5, and 10 kbp DNA, respectively. We note that the development of a detailed physical model to describe the combined diffusion-drift DNA dynamics as it approaches the nanopore is outside the scope of the current study and will be the subject of further publications. We nevertheless can take advantage of the longer optical time scales. Specifically, this offers two important benefits: (i) since the diffusion-drift dynamics of the DNA near the pore has much weaker dependency on the pore diameter than the translocation dwell time,[34] we expect that t_O is less influenced by the pore diameter or its shape, as compared with t_D, which is strongly affected by pore properties.[35] (ii) The longer optical dwell time effectively increases signal integration and therefore can be used to improve the signal-to-noise ratio (SNR) of the optical sensing.

A comparison of representative electro-optical events of DNA containing either 6, 7, or 21 M.*Taq*I sites (2.5, 5, and 10 kbp, respectively) is shown in Figure 3c. We observe two salient features: (1) The amplitude and dwell time of the optical signals clearly increase with increasing number of M.*Taq*I sites and length of the DNA. (2) The fully methylated ("+M.SssI") DNA did not produce an optical signal, as expected. To quantitatively compare the fluorescence signals between the methylated and unmethylated molecules, we extracted from each event the total number of photons that were detected during its transient through the nanopore (t_D). Additionally, our program evaluates the optical background level for each event, before its arrival to the pore, to obtain the net fluorescence counts. In order to avoid biasing of the results by the slow translocation events (essentially the tail of the t_D distributions shown in Figure 3b top panels), we normalize each of the events' photon sum by its residence time in the

DOI: 10.1021/acsnano.6b04748
ACS Nano 2016, 10, 8861−8870

pore. In this way each event contributes evenly to the photon sum histogram. Our results are presented in Figure 3d as semilog plots for the three different DNAs, along with the distribution of the background emission obtained in the beginning of the experiment, prior to the addition of the DNA sample. The data were fitted with a single Gaussian function for each case, allowing us to quantify the peak values of our statistical data sets (see Supporting Information for fit results). From this analysis we can define the optical signal gain as the ratio between the peak of the unmethylated sample and the methylated one. The values that we obtain for the three DNA lengths are ×5.1, ×8.0, and ×9.0 for the 2.5, 5, and 10 kbp DNA, respectively. Notably, the distributions of the background signals (gray bars and lines) nearly overlap with the corresponding one of the methylated DNA (except for the 10 kbp methylated sample, which produced slightly higher background, probably due to residual free dyes remaining after the nanopore alignment).

To establish a direct, quantitative correlation between the optical signal in each event and the number of M.*Taq*I sites, we corrected each DNA translocation event with its own optical background, measured just prior to the arrival of the DNA to the detection volume. This allowed us to measure the net photon sum of each event and calculate the net photon flux of each event by normalizing it by its optical dwell time t_O. This normalization was proven to be better than normalizing by the electrical dwell time t_D (as was done in Figure 3d) due to the longer integration time. Furthermore, it produced results that are practically insensitive to the exact nanopore size or membrane thickness. This insensitivity is significant since it is well known that nanopore size and thickness affect substantially the electrical dwell time and blocked current. Therefore, the optical signals permitted a more robust and quantitative comparison among the various DNA samples measured using slightly different nanopores. Our results are presented in Figure 4 and Table 1, showing the net photon flux histograms for the three −M.SssI samples. The histograms were fitted using Gaussian functions, from which we extract the peak values (I_{max}) and standard deviations. The inset of Figure 4 shows the values of I_{max} for the three DNA samples. Notably, as can be seen in Table 1, the contribution of each M.*Taq*I site to the

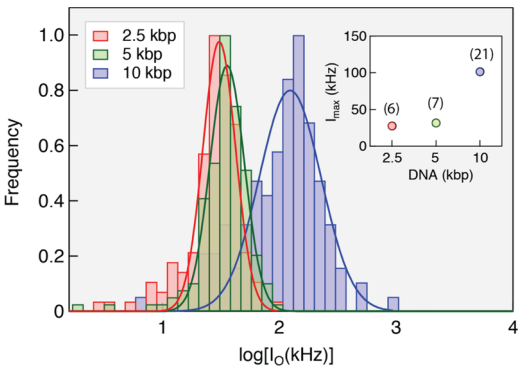

Figure 4. Comparison of the normalized TAMRA photon emission of the three DNA samples, as indicated. Semilog intensity histograms of the data yield well-defined peaks for the intensities approximated by Gaussian functions (solid lines). The inset shows the peaks (I_{max}) of the intensity for the three DNA lengths, also indicating the number of M.*Taq*I sites for each DNA. Notably, I_{max} scales precisely with the number of M.*Taq*I sites, not with DNA length (see also Table 1).

Table 1. Electro-optical Measurements of the Fluorescence Peak Intensities for Each of the TAMRA-Labeled DNAs and the Intensity per CpG within the M.*Taq*I Recognition Sites

DNA	# CpG	I_{max}	I_{max}/# CpG
2.5 kbp	6	27.5 ± 1.6	4.58 ± 0.27
5 kbp	7	31.6 ± 1.6	4.51 ± 0.23
10 kbp	21	101.4 ± 2.4	4.82 ± 0.12

overall signal is independent of the DNA sample used, yielding a constant value within the experimental variations of 4.60 ± 0.25 photons/ms and targeted CpG site.

The results presented in Figure 4 and in Table 1 suggest that optical detection of MTase-labeled DNA molecules using synthetic AdoMet analogues can be used to quantitatively measure the number of target CpG sites in random DNA samples. A comparison between the obtained photon count for the 2.5 and 5 kbp DNA having almost the same number of TCGA sites suggests that under the conditions used nonspecific labeling remains negligible, as the 2-fold longer 5 kbp DNA yields identical photon count *per* TCGA site to the 2.5 kbp DNA, within the experimental error. At the same time the fact that we received constant photon flux values per targeted CpG for all samples supports that the DNA samples are, by large, fully labeled. This is also supported by the protection of the DNA samples against fragmentation by R.*Taq*I (Figure 2b). Furthermore, despite the fact that the three molecules displayed much different diffusion and translocation dynamics (see Supporting Information), the photon normalization of each event individually removed these unavoidable thermal variations, allowing us to establish electro-optical nanopore sensing as a robust way for single-molecule quantification of unmethylated CpGs.

Multicolor Electro-optical Sensing for Orthogonal Site Labeling Quantification. Having established a proof of principle for labeling and single-molecule quantification of unmethylated sites, we seek to further expand the ability of the method for multiple colors. The ability to detect and quantify multiple colors simultaneously may open up the possibility to specifically target multiple, different recognition sequences, each one with its own specific DNA MTase and custom AdoMet analogue. In addition it may permit the coquantification of DNA methylation with other DNA modifications such as 5-hydroxymethylcytosine[36] or DNA damage lesions,[37] permitting a fully orthogonal labeling method for epigenetic biomarkers. For the sake of proof of principle demonstration we synthesized an additional AdoMet analogue coupled to the red fluorophore CF640R (AdoYnCF640R). The two AdoMet analogues were allowed to react simultaneously with the 10 kbp DNA (harboring 21 unmethylated M.*Taq*I sites) in the presence of M.*Taq*I, resulting in random but complete labeling of the DNA with the TAMRA and CF640R dyes. The DNA sample was analyzed using our nanopore system, excited simultaneously by two lasers (532 nm, 120 μW and 640 nm, 94 μW), and emission was acquired by two avalanche photodiodes (APDs) separated by a high-pass dichroic mirror (cutoff wavelength 650 nm), as detailed in the Methods section. In Figure 5a we present a representative set of events obtained in this experiment: each electrical DNA translocation event (blue curve) is accompanied by bursts of photons in both the "green" (TAMRA) and "red" (CF640R) detectors, indicating that our samples are labeled with both fluorophores. Bulk gel analysis of

DOI: 10.1021/acsnano.6b04748
ACS Nano 2016, 10, 8861−8870

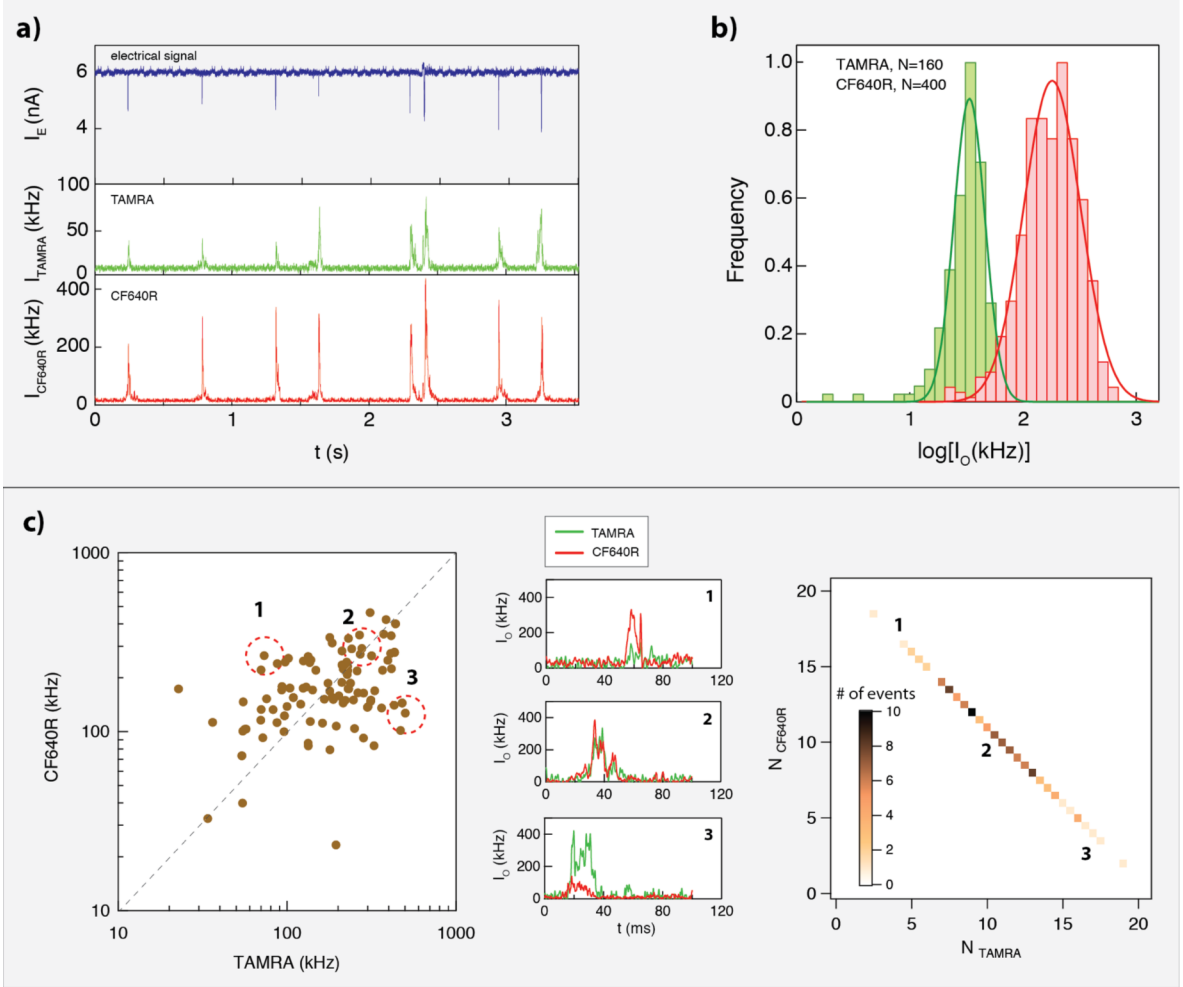

Figure 5. Two-color sensing of M.*Taq*I-labeled 10 kbp DNA. (a) Typical electrical (blue) and optical (green, TAMRA channel and red, CF640R channel) events. The time between events was removed for display purposes. (b) Intensity calibration of the green and red channels is performed by acquiring TAMRA-only or CF640R-only labeled 5 kbp DNA events. The two histograms corresponding to the two colors are shown (the number of events is indicated in each case). The ratio of the peak values is used to calibrate the brightness and detection efficiency ratio between the two channels. (c) Left: Normalized counts scatter plot of 115 individual events. Middle: Three representative dual-color intensity traces (indicated by numbers) for different TAMRA/CF640R ratios. Right: Using the intensity calibration we can evaluate the number of TAMRA *versus* CF640R labels on each DNA molecule. The two-dimensional histogram of the data displays the occurrences of DNA molecules with specific TAMRA and CF640R labels.

the sample (shown in the Supporting Information) confirmed the dual labeling.

From examination of the dual-color translocation events it is apparent that the CF640R photons' burst intensities are substantially stronger than those associated with TAMRA. There could be two possible reasons for this: first, this could be due to a strong bias in the labeling with AdoYnCF640R over AdoYnTAMRA. However, this option is unlikely since in preliminary studies we observed that M.*Taq*I has a roughly 4-fold lower activity with AdoYnCF640R compared to AdoYnTAMRA, and thus we used an excess of the red over the green cofactor (3:1) in the two-color labeling reaction to adjust the two reactivities. Second, which was later confirmed, is that the molecular brightness of the CF640R (multiplication of its specific absorption and quantum yield) and the detection efficiency of its emission path in our electro-optical apparatus are substantially higher as compared with the one associated with the TAMRA channel. To calibrate the ratio of fluorophore brightnesses and detection efficiencies between the two channels, we used M.*Taq*I and AdoYnCF640R to label the 5 kbp DNA fragment as used in Figure 3 and translocated the sample using a 4 nm pore and excitation laser of 640 nm with an intensity of 94 μW (representative events are shown in the Supporting Information). We utilized the normalization method discussed in Figure 4 to obtain net photon flux intensity using CF640R in the red emission channel. First we corrected the leakage of the TAMRA fluorescence to the red channel by calculating the ratio between the green and red APD signals obtained for the translocation of the 10 kbp DNA fragment used in Figure 3. Next we compared the TAMRA (green) and CF640R (red) labeling of the 5 kbp DNA (results are shown in Figure 5b). From fitting the histogram with Gaussian functions we obtained peaks at 31.6 and 169.4 kHz for TAMRA and CF640R, respectively. These results allow us to normalize the TAMRA/CF640R counts in the system such that their relative levels for each translocation event are unbiased by the detection efficiencies or fluorophore brightness, and hence the relative intensities ratio represents the labeling ratio with the two AdoMet analogues.

DOI: 10.1021/acsnano.6b04748
ACS Nano 2016, 10, 8861−8870

In Figure 5c we display a scatter plot of the brightness/detection efficiency corrected distribution of the randomly labeled 10 kbp DNA. We first note that most of the events fall around the diagonal line, showing that, on average, the DNA molecules are equally labeled with AdoYnTAMRA and AdoYnCF640R. Three representative two-color optical events from different areas are shown illustrating either heavier CF640R labeling, almost equal labeling, and heavier TAMRA labeling (indicated by "1", "2", and "3", respectively). Notably, with the corrected intensities of the two colors we can calculate the number of AdoYnTAMRA and AdoYnCF640R in each translocation event. These data are shown as a two-dimensional histogram (Figure 5c right panel) where the color indicates the number of DNA molecules in our data with the specific numbers of the AdoYnTAMRA and AdoYnCF640R labels.

CONCLUSIONS

We present a proof of principle study of a labeling and single-molecule quantification method for multiple 5-methylcytosines. Our method involves a single-step covalent coupling of DNA with synthetic AdoMet analogues using DNA MTases followed by molecule-by-molecule nanopore quantification with a single or multiple colors. Two distinct features of the DNA MTase labeling method set it aside from other single-molecule epigenetic sensing methods, offering potential advantages for broader use of the method using clinical samples: First, the availability of different CpG-methylation-sensitive DNA MTases permits targeting of either frequent or rare sequence motifs in the genome, with the development of the appropriate AdoMet analogues.[38] For example, some DNA MTases (*i.e.*, M.SssI) target each unmethylated CpG site, located in any sequence context, while other DNA MTases mainly recognize sequences of 4 or 6 specific nucleotides. Therefore, our method offers the possibility to serially perform multiple, orthogonal, labeling reactions each targeting its own specific sequence and color, followed by the single-molecule quantification of each DNA MTase activity. Second, unlike MBDs, the DNA MTase labeling reaction occurs only if the cytosine in the target CpG site is not methylated. This permits targeting hypomethylated sites in the genome, such as promoter regions in many of the oncogenes, which are currently considered to be an extremely important biomedical target.

In this study we show that an electro-optical nanopore sensing of DNA MTase labeled DNA can yield highly quantitative results, allowing us to detect fully methylated DNA molecules (electrical signal but no optical signal), partially methylated DNA (electrical and optical signals), and achieve a calibrated scale to count the number of unmethylated CpGs in the target sequences in each DNA molecule. Two-color sensing demonstrated in Figure 5 opens up the possibility to include multiple DNA MTases and achieve orthogonal labeling/sensing of 5-methylcytosines, as well as other epigenetic biomarkers, present in highly specific DNA recognition motifs.

METHODS

Nanochip Fabrication and Assembly for Electro-optical Sensing. The nanochip fabrication process and further details of the electro-optical cell are provided in the Supporting Information. Briefly, reactive ion etching (RIE) is used to locally thin 3 μm diameter wells in the 50 nm thick low-stress SiN_x deposited on a silicon wafer substrate to roughly 15 nm. Back-side alignment and RIE are then used to create a hard mask square pattern on the back side of the wafer, such that the front-side well pattern is centered with the hard mask pattern. Free-standing SiN_x membranes of size ranging from 10 to 25 μm square were created by anisotropic KOH wet etch. A schematic illustration of the chip and a white light optical micrograph of the membrane/well area of a typical device are shown in Figure 6a and b, respectively. Nanopores are drilled in the thin circular region of each of the SiN_x films by focusing an electron beam using a high-resolution transmission electron microscope (Titan FEI TEM).

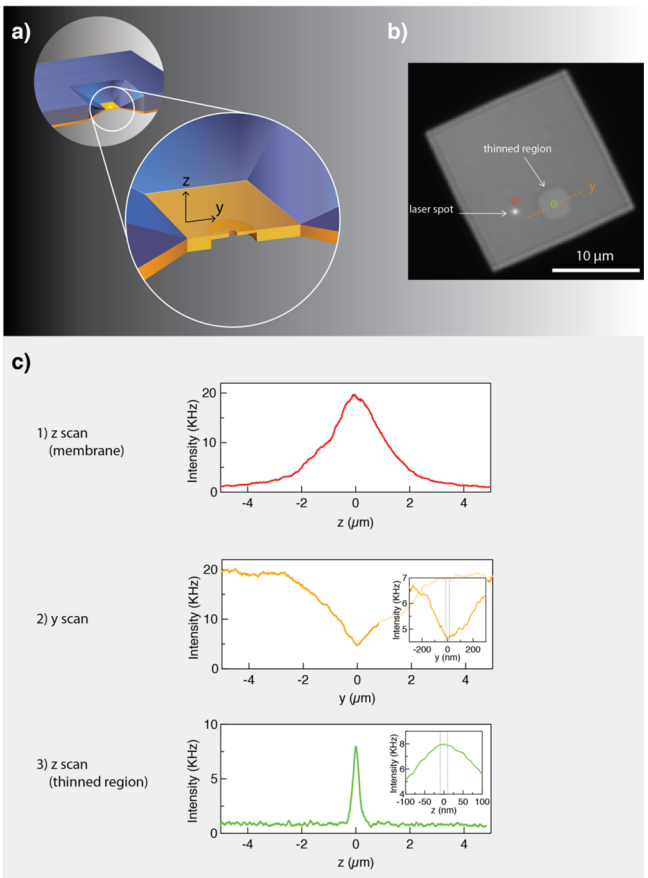

Figure 6. Schematic illustration of the nanopore device optical image of the membrane- and nanopore-positioning steps. (a) Chip configuration containing free SiN_x membrane with a thinner region in the middle. (b) White light optical image of the SiN_x membrane, showing the ~3 μm thinned region. The laser spot can be seen on the membrane (white spot). Red and green circles represent the *z*-scan position, and the yellow line represents the *y*-scan path. (c) Results from the three scans, to obtain optimal nanochip alignment at the confocal spot.

The drilled pores are hydrated, mounted onto a custom-made Teflon holder, immersed in buffer, and placed in a homemade cell equipped with a quartz cover-slide bottom. The nanochip cell is mounted on a 3D nanopositioner stage capable of performing nanometer movements and is electrically shielded by a properly grounded homemade copper box. The entire setup is mounted on a vibration-isolating optical table.

For the optical sensing a custom-made confocal microscope was constructed. Briefly, two collimated laser lines are focused to a diffraction-limited spot at the nanopore position. The emitted light is collected by the same objective, focused onto a spatial pinhole to reject out-of-focus light, and directed onto two spectrally separated APDs for two-color imaging. The ion current flowing through the pore is measured using the two Ag/AgCl electrodes connected to a high-bandwidth amplifier (Axon 200B) and filtered at 10 kHz. For data acquisition we used two data acquisition boards: NI-6211 DAQ for

DOI: 10.1021/acsnano.6b04748
ACS Nano 2016, 10, 8861−8870

analog signal acquisition and for applying the voltage bias sampled at 125 kHz, and NI-6602 for photon counting sampled at 500 kHz. The two cards were triggered simultaneously *via* a hardware connection and were fully controlled by a custom LabVIEW program.

Experimental Flow, Nanopore Alignment, and Data Analysis. The locally thinned, TEM-drilled, chips allow us to substantially reduce the optical background emanated by the membrane, hence increasing the SNR of the optical measurements. In addition, this chip configuration highly facilitates the accurate positioning of the nanopore at the confocal laser spot, taking advantage of the fact that the photoluminescence (PL) emanated by the SiN_x is strongly suppressed at thinned membrane areas, as well as in those areas that are exposed to strong e-beam intensities during pore drilling.[27] An alignment procedure was carefully performed prior to each experiment, including the following steps: First, white light illumination was used to coarsely align the 3 μm well and the laser spot in the z direction (Figure 6 b). Then, three scans were performed using the nanopositioner to determine the optimal alignment in 3D. In each case the PL was recorded during the scans (Figure 6c). In step 1, a z-scan was performed outside the thin region (marked with a red circle in Figure 6b) to obtain the rough membrane position in the z-direction, indicated by a clear peak in the scan (red curve). In step 2, the z-position was fixed to the value where the highest PL was detected in step 1, and the membrane was scanned in the $x-y$ dimensions, looking for the point with the minimal PL value. Figure 6c,2 presents a y-scan of the thin region (scan path is presented by a yellow line in Figure 6b) in which a clear minimum in the PL is detected with nanometric precision. A scan in the x-axis was performed similarly to the y-axis (not shown). In step 3, the $x-y$ position was fixed to the point with the lowest PL (green circle in Figure 6b), and a second z-scan was performed using finer resolution, looking again for the maximum PL representing the membrane position in the z-dimension (Figure 6c,3). As can be seen in the inset of Figure 3c (bottom panel), the membrane location is determined with roughly ±10 nm resolution in z, marked by a dashed rectangle.

In a typical experiment ~10 pM of DNA molecules was introduced into the *cis* chamber. Theoretically in this concentration range <1 molecule resides on average in the confocal volume. This yielded a low optical background that enables single-fluorophore sensing with high SNR. Each experiment starts by recording both the open-pore current of the nanopore and the optical background before adding the DNA. Then the unmethylated, labeled, DNA sample is added to the *cis* chamber, and the electrical and optical signals of the translocation events are recorded. Next the chamber was thoroughly washed and the same pore was used to translocate the methylated, unlabeled, sample. As a labeled DNA molecule reached the confocal volume, an abrupt increase in the optical signal was observed (see Figure 1 and Figure 5). Synchronization of the electrical and optical signals allowed us to reject events where DNA molecules approach the nanopore, but did not translocate through ("unsuccessful translocation") or a small fraction of electrical-only events. Throughout the experiments our program detected electrical translocation events according to threshold parameters set by the user. The electrical events, padded from both sides, were saved simultaneously, with the optical signal detected at the same time.

For data analysis an offline program reads each event at the time from the electrical signal and analyzes it to extract its dwell time (t_D), the amplitude drop ($I_B = i_{block}/i_{open}$), start time (t_{start}), and end time (t_{end}). Next, the optical signal extracted from the exact same temporal section is analyzed in the following manner: first the optical data between t_{start} and t_{end} is extracted and integrated to obtain the average number of photons emitted during the electrical event. Then a second analysis is performed according to optical threshold parameters set by the user to obtain the start time and end times of the optical signals as well as the optical dwell time, t_O (see Figure 3a and Supporting Information).

Sample Preparation and Validation. For the validation experiment 5 μg of DNA (No Limit, Thermo Scientific) at 0.5 μg/μL was divided into two equal samples. The first sample was methylated using M.SssI (Thermo Scientific) by treating it with 80 μM *S*-adenosyl-L-methionine (New England Biolabs) in M.SssI reaction buffer (10 mM Tris-HCl, pH 7.5, 10 mM $MgCl_2$, 0.1 mg/mL BSA) at a total volume of 30 μL, for 1 h at 37 °C. The reaction was stopped by heating to 65 °C for 30 min. To remove the residual cofactor, we performed ethanol precipitation using standard protocols. The pellets were vacuum-dried and resuspended in 5 μL of double-distilled water.

The methylated and unmethylated DNA samples were then treated with M.*Taq*I and AdoYnTAMRA (or AdoYnCF40R). Labeling reactions were carried out as follows: roughly 2.5 μg of DNA was dissolved in a buffer containing 50 mM KOAc, 20 mM Tris-HOAc, pH 7.9, 10 mM $MgOAc_2$, 1 mM DTT, 0.01% by volume Triton X-100, 100 μg/mL BSA, and AdoYnTAMRA (40 μM final concentration, prepared in house) as well as 10 equiv of M.*Taq*I per TCGA site. Reactions were performed at a total volume of 25 μL for 2.5 h at 65 °C. Reactions were stopped by adding 40 μg of proteinase K (20 μg/μL) (Thermo Scientific) and incubation for 1 h at 45 °C. To remove the residual cofactor, we performed ethanol precipitation using standard protocols. After washing the pellet five times with 70% ethanol it was vacuum-dried and resuspended in 20 μL of DDW for UV−vis absorption quantification. Two-color labeling was performed similarly to the one-color labeling,; however since we find that M.*Taq*I has a slight preference for AdoYnTAMRA over AdoYnCF640R, we used a 10 μM final concentration of AdoYnTAMRA and 30 μM AdoYnCF640R.

Validation of the prepared DNA samples was performed as follows: 300 ng of TAMRA-labeled DNA or 300 ng of M.SssI-methylated DNA was treated with 1 μL of 10 U/μL R.*Taq*I restriction enzyme (Thermo Scientific) in 10 μL of R.*Taq*I buffer. The samples were incubated for 3 h at 65 °C. The reactions were stopped by adding 0.5 M EDTA, pH 8.0, to a final concentration of 20 mM. Then 2 μL of 6× electrophoresis loading buffer (50 mM Tris, 60 mM EDTA, 60% glycerol) was added, and the samples were loaded on a 0.8% agarose gel. Samples were allowed to run for 90 min at 100 V and then imaged using a 532 nm laser gel scanner (GE Healthcare, Typhoon) followed by SYBR Gold staining (30 min) and reimaging.

ASSOCIATED CONTENT

Supporting Information

The Supporting Information is available free of charge on the ACS Publications website at DOI: 10.1021/acsnano.6b04748.

Positions of M.*Taq*I recognition sites on the three DNA double strands, DNA sample preparation procedures and bulk characterization, nanochip fabrication for electro-optical sensing, data acquisitions and analysis of electro-optical events, experimental setup, fits for the semilog plots, electrical scatter plots, representative electro-optical traces of 5 kbp DNA labeled with CF640R (PDF)

AUTHOR INFORMATION

Corresponding Authors

*E-mail: uv@post.tau.ac.il.

*E-mail: ameller@technion.ac.il.

Author Contributions

#T. Gilboa and C. Torfstein contributed equally to this work.

Notes

The authors declare no competing financial interest.

ACKNOWLEDGMENTS

We are grateful to A. H. Squires for careful reading and commenting on the manuscript, to O. Assad for his kind assistance in the nanopore device fabrication, and to K. Glensk for preparing the M.*Taq*I enzyme. We acknowledge financial support from the Umbrella cooperation (A.M. and E.W.), the BeyondSeq consortium (EC program 63489 to A.M. and Y.E.),

DOI: 10.1021/acsnano.6b04748
ACS Nano 2016, 10, 8861−8870

the German-Israeli Foundation [I-1196-195.9/2012] (E.W. and Y.E.), the European Research Councils starter grant [337830] (Y.E.), and i-Core program of the Israel Science Foundation (1902/12 to A.M. and Y.E.).

REFERENCES

(1) Chen, Z. X.; Riggs, A. D. DNA Methylation and Demethylation in Mammals. *J. Biol. Chem.* **2011**, *286*, 18347−18353.

(2) Smith, Z. D.; Meissner, A. DNA Methylation: Roles in Mammalian Development. *Nat. Rev. Genet.* **2013**, *14*, 204−220.

(3) Landan, G.; Cohen, N. M.; Mukamel, Z.; Bar, A.; Molchadsky, A.; Brosh, R.; Horn-Saban, S.; Zalcenstein, D. A.; Goldfinger, N.; Zundelevich, A.; Gal-Yam, E. N.; Rotter, V.; Tanay, A. Epigenetic Polymorphism and the Stochastic Formation of Differentially Methylated Regions in Normal and Cancerous Tissues. *Nat. Genet.* **2012**, *44*, 1207−1214.

(4) Landau, D. A.; Clement, K.; Ziller, M. J.; Boyle, P.; Fan, J.; Gu, H.; Stevenson, K.; Sougnez, C.; Wang, L.; Li, S.; Kotliar, D.; Zhang, W.; Ghandi, M.; Garraway, L.; Fernandes, S. M.; Livak, K. J.; Gabriel, S.; Gnirke, A.; Lander, E. S.; Brown, J. R.; et al. Locally Disordered Methylation Forms the Basis of Intratumor Methylome Variation in Chronic Lymphocytic Leukemia. *Cancer Cell* **2014**, *26*, 813−825.

(5) Laird, P. W. Principles and Challenges of Genome-Wide DNA Methylation Analysis. *Nat. Rev. Genet.* **2010**, *11*, 191−203.

(6) Korlach, J.; Turner, S. W. Going Beyond Five Bases in DNA Sequencing. *Curr. Opin. Struct. Biol.* **2012**, *22*, 251−261.

(7) Clark, T. A.; Lu, X.; Luong, K.; Dai, Q.; Boitano, M.; Turner, S. W.; He, C.; Korlach, J. Enhanced 5-Methylcytosine Detection in Single-Molecule, Real-Time Sequencing *Via* Tet1 Oxidation. *BMC Biol.* **2013**, *11*, 4.

(8) Wanunu, M.; Meller, A. Single-Molecule Analysis of Nucleic Acids and DNA-Protein Interactions Using Nanopores. In *Single-Molecule Techniques: A Laboratory Manual*; Selvin, P., Ha, T. J., Eds.; Cold Spring Harbor Laboratory Press: New York, 2008; pp 395−420.

(9) Dekker, C. Solid-State Nanopores. *Nat. Nanotechnol.* **2007**, *2*, 209−215.

(10) Meller, A. Nanopores: Single-Molecule Sensors of Nucleic Acid-Based Complexes. In *Advances in Chemical Physics*; John Wiley & Sons, Inc.: Hoboken, 2012; pp 251−268.

(11) Laszlo, A. H.; Derrington, I. M.; Ross, B. C.; Brinkerhoff, H.; Adey, A.; Nova, I. C.; Craig, J. M.; Langford, K. W.; Samson, J. M.; Daza, R.; Doering, K.; Shendure, J.; Gundlach, J. H. Decoding Long Nanopore Sequencing Reads of Natural DNA. *Nat. Biotechnol.* **2014**, *32*, 829−833.

(12) Jain, M.; Fiddes, I. T.; Miga, K. H.; Olsen, H. E.; Paten, B.; Akeson, M. Improved Data Analysis for the Minion Nanopore Sequencer. *Nat. Methods* **2015**, *12*, 351−356.

(13) Wanunu, M. Nanopores: A Journey Towards DNA Sequencing. *Physics of Life Reviews* **2012**, *9*, 125−158.

(14) Storm, A. J.; Chen, J. H.; Ling, X. S.; Zandbergen, H. W.; Dekker, C. Fabrication of Solid-State Nanopores with Single-Nanometre Precision. *Nat. Mater.* **2003**, *2*, 537−540.

(15) Kim, M. J.; Wanunu, M.; Bell, D. C.; Meller, A. Rapid Fabrication of Uniformly Sized Nanopores and Nanopore Arrays for Parallel DNA Analysis. *Adv. Mater.* **2006**, *18*, 3149−3153.

(16) Singer, A.; Rapireddy, S.; Ly, D. H.; Meller, A. Electronic Barcoding of a Viral Gene at the Single-Molecule Level. *Nano Lett.* **2012**, *12*, 1722−1728.

(17) Squires, A.; Atas, E.; Meller, A. Nanopore Sensing of Individual Transcription Factors Bound to DNA. *Sci. Rep.* **2015**, *5*, 11643.

(18) Feng, J.; Liu, K.; Bulushev, R. D.; Khlybov, S.; Dumcenco, D.; Kis, A.; Radenovic, A. Identification of Single Nucleotides in Mos2 Nanopores. *Nat. Nanotechnol.* **2015**, *10*, 1070−1076.

(19) Zahid, O. K.; Zhao, B. S.; He, C.; Hall, A. R. Quantifying Mammalian Genomic DNA Hydroxymethylcytosine Content Using Solid-State Nanopores. *Sci. Rep.* **2016**, *6*, 29565.

(20) Shim, J.; Humphreys, G. I.; Venkatesan, B. M.; Munz, J. M.; Zou, X. Q.; Sathe, C.; Schulten, K.; Kosari, F.; Nardulli, A. M.; Vasmatzis, G.; Bashir, R. Detection and Quantification of Methylation in DNA Using Solid-State Nanopores. *Sci. Rep.* **2013**, *3*, 1389.

(21) McNally, B.; Singer, A.; Yu, Z. L.; Sun, Y. J.; Weng, Z. P.; Meller, A. Optical Recognition of Converted DNA Nucleotides for Single-Molecule DNA Sequencing Using Nanopore Arrays. *Nano Lett.* **2010**, *10*, 2237−2244.

(22) Sawafta, F.; Clancy, B.; Carlsen, A. T.; Huber, M.; Hall, A. R. Solid-State Nanopores and Nanopore Arrays Optimized for Optical Detection. *Nanoscale* **2014**, *6*, 6991−6996.

(23) Anderson, B. N.; Assad, O. N.; Gilboa, T.; Squires, A. H.; Bar, D.; Meller, A. Probing Solid-State Nanopores with Light for the Detection of Unlabeled Analytes. *ACS Nano* **2014**, *8*, 11836−11845.

(24) Ivankin, A.; Henley, R. Y.; Larkin, J.; Carson, S.; Toscano, M. L.; Wanunu, M. Label-Free Optical Detection of Biomolecular Translocation through Nanopore Arrays. *ACS Nano* **2014**, *8*, 10774−10781.

(25) Gilboa, T.; Meller, A. Optical Sensing and Analyte Manipulation in Solid-State Nanopores. *Analyst* **2015**, *140*, 4733−4747.

(26) Yamazaki, H.; Ito, S.; Esashika, K.; Saiki, T. Optical Observation of DNA Motion During and Immediately after Nanopore Translocation. *Appl. Phys. Express* **2016**, *9*, 017001.

(27) Assad, O. N.; Di Fiori, N.; Squires, A. H.; Meller, A. Two Color DNA Barcode Detection in Photoluminescence Suppressed Silicon Nitride Nanopores. *Nano Lett.* **2015**, *15*, 745−752.

(28) Roberts, R. J.; Vincze, T.; Posfai, J.; Macelis, D. Rebase–a Database for DNA Restriction and Modification: Enzymes, Genes and Genomes. *Nucleic Acids Res.* **2010**, *38*, 234−236.

(29) Klimasauskas, S.; Weinhold, E. A New Tool for Biotechnology: Adomet-Dependent Methyltransferases. *Trends Biotechnol.* **2007**, *25*, 99−104.

(30) Hanz, G. M.; Jung, B.; Giesbertz, A.; Juhasz, M.; Weinhold, E. Sequence-Specific Labeling of Nucleic Acids and Proteins with Methyltransferases and Cofactor Analogues. *J. Visualized Exp.* **2014**, e52014.

(31) Gottfried, A.; Weinhold, E. Sequence-Specific Covalent Labelling of DNA. *Biochem. Soc. Trans.* **2011**, *39*, 623−628.

(32) Nelson, M.; McClelland, M. Site-Specific Methylation: Effect on DNA Modification Methyltransferases and Restriction Endonucleases. *Nucleic Acids Res.* **1991**, *19*, 2045−2071.

(33) Grunwald, A.; Dahan, M.; Giesbertz, A.; Nilsson, A.; Nyberg, L. K.; Weinhold, E.; Ambjornsson, T.; Westerlund, F.; Ebenstein, Y. Bacteriophage Strain Typing by Rapid Single Molecule Analysis. *Nucleic Acids Res.* **2015**, *43*, e117.

(34) Wanunu, M.; Morrison, W.; Rabin, Y.; Grosberg, A. Y.; Meller, A. Electrostatic Focusing of Unlabelled DNA into Nanoscale Pores Using a Salt Gradient. *Nat. Nanotechnol.* **2010**, *5*, 160−165.

(35) Carson, S.; Wilson, J.; Aksimentiev, A.; Wanunu, M. Smooth DNA Transport through a Narrowed Pore Geometry. *Biophys. J.* **2014**, *107*, 2381−2393.

(36) Michaeli, Y.; Shahal, T.; Torchinsky, D.; Grunwald, A.; Hoch, R.; Ebenstein, Y. Optical Detection of Epigenetic Marks: Sensitive Quantification and Direct Imaging of Individual Hydroxymethylcytosine Bases. *Chem. Commun.* **2013**, *49*, 8599−8601.

(37) Zirkin, S.; Fishman, S.; Sharim, H.; Michaeli, Y.; Don, J.; Ebenstein, Y. Lighting up Individual DNA Damage Sites by *in Vitro* Repair Synthesis. *J. Am. Chem. Soc.* **2014**, *136*, 7771−7776.

(38) Kriukiene, E.; Labrie, V.; Khare, T.; Urbanaviciute, G.; Lapinaite, A.; Koncevicius, K.; Li, D.; Wang, T.; Pai, S.; Ptak, C.; Gordevicius, J.; Wang, S. C.; Petronis, A.; Klimasauskas, S. DNA Unmethylome Profiling by Covalent Capture of Cpg Sites. *Nat. Commun.* **2013**, *4*, 2190.

DOI: 10.1021/acsnano.6b04748
ACS Nano 2016, 10, 8861−8870